1521-009X/47/10/1050–1060$35.00
Drug Metabolism and Disposition

https://doi.org/10.1124/dmd.119.087973
Drug Metab Dispos 47:1050–1060, October 2019

Prediction of Tissue-Plasma Partition Coefficients Using Microsomal Partitioning: Incorporation into Physiologically based Pharmacokinetic Models and Steady-State Volume of Distribution Predictions

Kimberly Holt, Min Ye, Swati Nagar, and Ken Korzekwa

Department of Pharmaceutical Sciences, Temple University School of Pharmacy, Philadelphia, Pennsylvania

Received May 13, 2019; accepted July 9, 2019

ABSTRACT

Drug distribution is a necessary component of models to predict human pharmacokinetics. A new membrane-based tissue-plasma partition coefficient (K_p) method ($K_{p,mem}$) to predict unbound tissue to plasma partition coefficients (K_{pu}) was developed using in vitro membrane partitioning [fraction unbound in microsomes (f_{um})], plasma protein binding, and log *P*. The resulting K_p values were used in a physiologically based pharmacokinetic (PBPK) model to predict the steady-state volume of distribution (V_{ss}) and concentration-time (C-t) profiles for 19 drugs. These results were compared with K_p predictions using a standard method [the differential phospholipid K_p prediction method ($K_{p,dPL}$)], which differentiates between acidic and neutral phospholipids. The $K_{p,mem}$ method was parameterized using published rat K_{pu} data and tissue lipid composition. The K_{pu} values were well predicted with $R^2 = 0.8$. When used in a PBPK model, the V_{ss} predictions were within 2-fold error for 12 of 19 drugs for $K_{p,mem}$ versus 11 of 19 for $K_{p,dPL}$. With one outlier removed for $K_{p,mem}$ and two for $K_{p,dPL}$, the V_{ss} predictions for R^2 were 0.80 and 0.79 for the $K_{p,mem}$ and $K_{p,dPL}$ methods, respectively. The C-t profiles were also predicted and compared. Overall, the $K_{p,mem}$ method predicted the V_{ss} and C-t profiles equally or better than the $K_{p,dPL}$ method. An advantage of using f_{um} to parameterize membrane partitioning is that f_{um} data are used for clearance prediction and are, therefore, generated early in the discovery/development process. Also, the method provides a mechanistically sound basis for membrane partitioning and permeability for further improving PBPK models.

SIGNIFICANCE STATEMENT

A new method to predict tissue-plasma partition coefficients was developed. The method provides a more mechanistic basis to model membrane partitioning.

Introduction

The volume of distribution and clearance equally determine the half-life of a drug. The steady-state volume of distribution (V_{ss}) can be predicted using empirical methods (Obach et al., 1997), computational approaches (Ghafourian et al., 2004; Lombardo et al., 2006; Zhivkova and Doytchinova, 2012), physiologic equations (Oie and Tozer, 1979; Lombardo et al., 2004; Korzekwa and Nagar, 2017a), and tissue:plasma partition coefficients (K_p). The K_p prediction methods are widely used since they describe the distribution in physiologically based pharmacokinetic (PBPK) models. While some methods require an in vivo component (Arundel, 1997; Björkman, 2002; Jansson et al., 2008; Poulin and Theil, 2009), others use more readily available in vitro inputs.

Several factors influence drug distribution, including partitioning into membranes and other lipids, binding to proteins (primarily plasma proteins), pH partitioning (e.g., lysosomes), transporters, and membrane permeability. Most models represent tissue interactions with in vitro surrogates. The Poulin and Krishnan (1995) model originally described phospholipid partitioning with the octanol:water partition coefficient (*P*) and assumed phospholipid composition to be represented by 30% octanol and 70% water. They developed K_p prediction equations that included an additional surrogate for neutral lipid partitioning in adipose tissue (Poulin and Theil, 2000; Poulin et al., 2001), which was modified by Berezhkovskiy (2004). Rodgers and Rowland (2006) developed two equations for prediction of unbound K_p (K_{pu}): one for acids, neutrals, and weak bases, and another for moderate-to-strong bases (Rodgers et al., 2005). Drug partitioning into erythrocytes was used to parameterize the interaction of bases with acidic phospholipids (APs). It was assumed that ionized bases interact only with APs, while uncharged molecules interact only with neutral phospholipids (Rodgers et al., 2005; Rodgers and Rowland, 2006).

In most currently used composition-based models, log *P* is used to model the phospholipid partitioning (0.3*P*). A shortcoming of using log *P* to represent phospholipid partitioning is the lack of orientation-specific interactions with phospholipid membranes (Balaz, 2009; Nagar and Korzekwa, 2012, 2017). Additionally, both neutral and ionized

This research was supported by the National Institutes of Health [Grants R01GM104178 and R01GM114369].
https://doi.org/10.1124/dmd.119.087973.

ABBREVIATIONS: AAFE, absolute average fold error; AP, acidic phospholipid; AUC, area under the curve; BC, blood cell; BP, blood to plasma; C-t, concentration-time; EOC, exposure overlap coefficient; f_{ew}, fractional volume of extracellular water; f_{iw}, fractional volume of intracellular water; f_{nl}, fractional volume of neutral lipids; f_{um}, fraction unbound in microsomes; f_{up}, fraction unbound in plasma; K_p, tissue:plasma partition coefficient; $K_{p,dPL}$, differential phospholipid tissue-plasma partition coefficient prediction method; $K_{p,mem}$, membrane-based tissue-plasma partition coefficient prediction method; K_{pu}, unbound tissue:plasma partition coefficient; *P*, octanol:water partition coefficient; PBPK, physiologically based pharmacokinetic; $pK_{a,a}$, ionization constant for acids; $pK_{a,b}$, ionization constant for bases; V_{ss}, steady-state volume of distribution.

bases are known to interact with all phospholipids, and not just net-neutral and net-acidic phospholipids, respectively. Therefore, current methods to calculate K_p appear to be based on mechanistically unsound assumptions. Previously, we used microsomal partitioning [fraction unbound in microsomes (f_{um})] instead of log P to parameterize phospholipid partitioning in a V_{ss} model (Korzekwa and Nagar, 2017a). Partitioning into microsomes (unsorted phospholipid vesicles) is used extensively in clearance predictions and can be determined experimentally or predicted (Austin et al., 2002; Hallifax and Houston, 2006; Poulin and Haddad, 2011; Nagar and Korzekwa, 2017). A benefit of using f_{um} to represent phospholipid partitioning is that it measures interactions with all phospholipids for both charged and uncharged species.

Previous studies have compared different K_p prediction methods and their ability to predict both tissue K_p and/or V_{ss} (De Buck et al., 2007; Poulin and Theil, 2009; Jones et al., 2011; Graham et al., 2012; Zou et al., 2012; Chan et al., 2018). These studies came to different conclusions on the most accurate K_p model, which was primarily dependent on the drug data set used (De Buck et al., 2007; Graham et al., 2012). Graham et al. (2012) showed that the Rodgers et al. (2005) method was able to better predict K_p and V_{ss} for different classes of drugs than other composition-based models. The Poulin and Theil (2009) method led to good V_{ss} predictions, but required in vivo data (K_{pu} muscle) (Graham et al., 2012). More recently, Chan et al. (2018) compared the ability of composition-based K_p models and preclinical extrapolation to predict V_{ss}. Composition-based models predicted V_{ss} with accuracy similar to preclinical extrapolation. They noted that the Rodgers method was able to predict V_{ss} well for drugs with log P values less than 3, and that many drugs with large errors in V_{ss} for composition-based models also had errors in preclinical extrapolation (Chan et al., 2018).

This report evaluates a model to predict K_p using f_{um} to represent membrane partitioning. Plasma protein binding and microsomal partitioning values were determined experimentally for 19 drugs. Tissue K_p values were calculated for each compound using a differential phospholipid K_p prediction method ($K_{p,dPL}$) (Rodgers et al., 2005; Rodgers and Rowland, 2006), as well as a method that uses f_{um} to parameterize membrane partitioning [the membrane-based K_p prediction method ($K_{p,mem}$)]. Simulations were run and their ability to predict V_{ss} and concentration-time (C-t) profiles was determined. More mechanistically sound assumptions for K_{pu} will be required when expanding current perfusion-limited PBPK models to include explicit membrane partitioning and permeability. Models to predict K_{pu} bases on experimental partitioning into membranes may allow a facile transition to models that limit permeability with explicit membrane compartments (Nagar et al., 2014).

Materials and Methods

Materials. A Harvard Apparatus (Holliston, MA) 96-well equilibrium dialyzer and single-plate Harvard Apparatus plate rotator were used for equilibrium dialysis experiments. Human plasma was obtained from US Biologic (Salem, MA) and Innovative Research Inc. (Novi, MI). Rat liver microsomes were obtained from BD Biosciences (San Jose, CA) and Corning Life Sciences (Tewksbury, MA). Warfarin, fluconazole, glyburide (glybenclamide), ketoprofen, fenofibrate, +/*cis*-diltiazem hydrochloride, +/− verapamil hydrochloride, caffeine, betaxolol hydrochloride, DMSO, nicardipine hydrochloride, metoprolol tartrate, felodipine, and nafcillin sodium were obtained from Sigma Aldrich (St. Louis, MO). Quinidine gluconate, formic acid, acetonitrile, and diphenhydramine hydrochloride were obtained from Fisher Scientific (Norristown, PA). Mibefradil hydrochloride was obtained from Cayman Chemical Company (Ann Arbor, MI). Diclofenac sodium was obtained from Calbiochem (Burlington, MA). Fenofibric acid was obtained from Kano Laboratories (Nashville, TN). One milligram per milliliter solutions of phenytoin, diazepam, and midazolam in methanol were obtained from Cerilliant (a Sigma Aldrich company). The 100 mM PBS and 0.3 mM $MgCl_2$ dialysis buffer was composed of magnesium hydrochloride hexahydrate (Fisher Scientific), potassium phosphate monobasic (Sigma Aldrich), and potassium phosphate dibasic (Fisher Scientific). An Agilent 1100 HPLC and API 4000 mass spectrometer and Agilent 1100 HPLC and API 4000 Q-Trip mass spectrometer were used to determine the concentrations for equilibrium dialysis. Mathematica version 11.0 (Wolfram, Champaign, IL) was used for all compartmental modeling and simulations. Literature data from plots were digitized using Engauge Plot Digitizer version 10.4 (GitHub, San Francisco, CA).

Probe Drug Selection and Data Collection. A diverse set of drugs made up of acids, bases, and neutrals was selected to compare the prediction methods (Table 1). Drugs were considered neutral when primarily uncharged at physiologic pH (7.4). Unless noted otherwise, the pK_a values of acids ($pK_{a,a}$) and bases ($pK_{a,b}$) for neutrals were set at 14 and 1, respectively. Any significant ionized and neutral fraction was considered by both methods. The probe drugs were selected based on

TABLE 1

Pharmacokinetic parameters of test drugs

Test Drug	Class	Type	Number of Subjects	Weight *kg*	Dose *mg*	Duration *min*	Number of Points	V_{ss} *l*	CL *l/h*	Reference
Betaxolol	B	Infusion	$n = 10$	73.6	8.94	30	17	360	11	Ludden et al., 1988
Diltiazem	B	Infusion	$n = 12$	63	15	30	13	306	97	Hermann et al., 1983
Diphenhydramine	B	Bolus	$n = 8$	98.0	56	N/A	12	788	43	Scavone et al., 1990
Metoprolol	B	Infusion	$n = 5$	66	3.9	10	20	274	59	Regårdh et al., 1974
Mibefradil	B	Infusion	$n = 6$	70[a]	20	30	16	187	17	Clozel et al., 1991
Nicardipine	B	Bolus	$n = 6$[b]	67.0	10	N/A	12	62	76	Campbell et al., 1985
Quinidine	B	Infusion	$n = 12$[b]	65.3	244	22	12	227	18.5	Ueda et al., 1976
Verapamil	B	Infusion	$n = 20$	70[a]	10	5	15	266	49	McAllister and Kirsten, 1982
Caffeine	N	Infusion	$n = 10$	79.5	350	30	17	42.8	5.2	Blanchard and Sawers, 1983
Diazepam	N	Infusion	$n = 24$	78.1	5	1	21	89.5	1.33	Agarwal et al., 2013
Felodipine	N	Infusion	$n = 10$	74	2.5	30	22	320	41.7	Edgar et al., 1985
Fluconazole	N	Infusion	$n = 6$	70[a]	50	N/A	13	59.3	1.25	Ripa et al., 1993
Midazolam	N	Bolus	$n = 6$	67.6	10	N/A	15	51.2	18	Heizmann et al., 1983
Phenytoin	N	Infusion	$n = 6$	78.1	275	6	15	38.8	1.76	Gugler et al., 1976
Diclofenac	A	Infusion	$n = 6$	65	46.5	2	15	9.23	17.6	Willis et al., 1980
Glyburide	A	Infusion	$n = 10$	77.8	2	60	19	11.78	4.88	Debruyne et al., 1987
Ketoprofen	A	Bolus	$n = 7$	70[a]	100	N/A	12	9.9	5.02	Debruyne et al., 1987
Nafcillin	A	Infusion	$n = 6$	70[a]	475	7	9	20.4	33.9	Waller et al., 1982
Warfarin	A	Bolus	$n = 6$	66.8	100	N/A	8	7.66	0.179	O'Reilly et al., 1971

A, acids; B, bases; N, neutral; CL, clearance.
[a]Individual weights not provided and 70 kg assumed.
[b]Individual C-t not provided. C-t profile simulated from average parameters.

the availability of literature intravenous pharmacokinetics data, as well as drug-specific parameters. Average experimental intravenous bolus and/or infusion C-t profiles for 19 drug studies were collected from the literature. If the data were represented as graphical C-t profiles, the plots were digitized. When average subject weight was available, simulations were conducted to reproduce the observed V_{ss} for that average weight. The observed clearance and the steady-state volume of distribution were determined by compartmental analysis using standard equations with Mathematica. Specifically, one- to three-compartment models were evaluated to generate the C-t profiles from the experimental data. Experimental clearance and V_{ss} values were determined from these compartmental models. The best model for the experimental data was determined by the corrected Akaike information criterion values (Akaike, 1974) and residual plots. For all drugs, microrate constants were well defined and use of noncompartmental analysis was not required. Experimental clearance values were assumed for all further modeling efforts and experimental V_{ss} values were compared with predicted values.

Literature physiologic data were used for K_p predictions and PBPK modeling (Brown et al., 1997; Poulin and Theil, 2002; Fenneteau et al., 2010; Ye et al., 2016). For drug-specific parameters [log *P*, pK_a, and blood to plasma (BP)] (Table 2), experimental values from the literature were preferred over calculated/predicted values, and if more than one experimental value was found, then the experimental values were averaged. Human BP values could not be found for betaxolol and nafcillin. For betaxolol, the values of the fraction unbound in plasma (f_{up}) were similar for rat and human; therefore, the rat BP value of 2.0 was used. For nafcillin, a value of 0.55 (1-hematocrit) was used, which is the BP ratio of similar compounds in humans (Greene et al., 1978). Also, this will not affect V_{ss} predictions since BP is not included in the K_p equations for acids. Protein binding was experimentally determined for all compounds (Table 2), with the exception of caffeine due to caffeine contamination in all plasma samples. A caffeine f_{up} value of 0.72 was determined by averaging values found in the literature.

The log P_{vo} (log of the vegetable oil:buffer partition coefficient) was calculated from log *P* using eq. 1 (Leo et al., 1971). This term is used to represent neutral lipid partitioning in adipose tissue in the $K_{p,dPL}$ method; however, it is not used in the $K_{p,mem}$ prediction method:

$$\log P_{vo} = 1.115 \cdot \log P - 1.35 \quad (1)$$

Microsomal Partitioning and Plasma Protein Binding. Equilibrium dialysis was used to determine the f_{up} and f_{um} for the probe drugs using a protocol modified from prior studies (Kochansky et al., 2008; Curran et al., 2011; Di et al., 2017). Human plasma was adjusted to pH 7.4 by adding 1 M HCl. For f_{um} determination, a 0.5 mg/ml rat liver microsomal solution was prepared from a 20 mg/ml pooled rat liver microsome stock solution. For highly bound compounds, a dilution method was used. Plasma was diluted using a 100 mM phosphate buffer and 3 mM $MgCl_2$ solution to either 50% or 10% plasma. A 50% dilution of plasma was used for warfarin, while a 10% dilution was used for ketoprofen, nicardipine, glyburide, diclofenac, felodipine, and mibefradil. Drug solutions (2 μM) in either plasma or microsomes were added to wells on one side of the dialyzer, and blank 100 mM phosphate buffer with 3 mM of $MgCl_2$ was added to the other side. The dialyzer plate was placed in the plate rotator, set to a speed of approximately 22 rotations per minute, and incubated for 22 hours at 37°C and 5% CO_2. Liquid chromatography–tandem mass spectrometry was used to determine the concentration of drug in the buffer and the matrix.

The fraction unbound in a given matrix was determined by dividing the concentration of drug on the buffer side by the concentration of drug on the matrix side. For protein binding experiments using the dilution method, the f_{up} value is calculated by eq. 2:

$$f_{up=} = \frac{1/D}{[(1/f_{u,d}) - 1] + 1/D} \quad (2)$$

where *D* is the dilution factor; $f_{u,d}$ is the fraction unbound in plasma measured in the diluted matrix; and f_{up} is the fraction unbound in plasma.

Experimental f_{um} values were measured at microsomal concentrations between 0.5 and 2 mg/ml and converted to values for 1 mg/ml (eq. 3) (Austin et al., 2002):

$$f_{u2} = \frac{1}{(C_2/C_1) \cdot [(1 - f_{u1})/f_{u1}] + 1} \quad (3)$$

where f_{u2} is the corrected unbound fraction; C_2 is the 1 mg/ml microsomal protein concentration; C_1 is the microsomal protein concentration used in assay; and f_{u1} is

TABLE 2

Drug-specific parameters

Compound	Class	f_{up} (n = 4)[a]	f_{um} (n = 4)[a]	Log *P*	p$K_{a,a}$	p$K_{a,b}$	BP	Log D_{vo}	CL *l/h*	Reference
Betaxolol	B	0.50 (12%)	0.77 (3%)	2.81	14	9.4	2[b]	1.78	10.2	Riddell et al., 1987; Recanatini, 1992; Rodgers and Rowland, 2007
Diltiazem	B	0.26 (8%)	0.48 (2%)	2.7	14	7.7	1	1.88	97.5	Rekker and Mannhold, 1992; Obach, 1999; Ishihama et al., 2002
Diphenhydramine	B	0.44 (4%)	0.84 (4%)	3.27	14	8.98	0.74	2.30	43	Albert et al., 1975; Sangster, 1994; Hansch et al., 1995; Obach, 1999
Metoprolol	B	0.87 (17%)	0.80 (3%)	1.88	14	9.7	1.14	0.746	58.8	Hansch et al., 1995; Rodgers and Rowland, 2007
Mibefradil	B	0.031 (11%)	0.034 (15%)	3.07	14	10.2	0.64	2.07	15.5	Welker et al., 1998; Nagar and Korzekwa, 2017
Nicardipine	B	0.0024 (7%)	0.039 (12%)	3.82	14	8.6	0.71	2.90	31.2	Sangster, 1993; Rodgers and Rowland, 2007
Quinidine	B	0.15 (8%)	0.815 (10%)	3.52	14	8.94	0.92	2.07	14	Sangster, 1994; Obach, 1999; Nagar and Korzekwa, 2017
Verapamil	B	0.088 (20%)	0.37 (19%)	3.79	14	8.92	0.74	2.88	49	Sangster, 1994; Hansch et al., 1995; Robinson and Mehvar, 1996; Obach, 1999
Caffeine	N	0.72[c]	0.98 (6%)	−0.07	14	1.04	1.01	−1.43	5.2	Hansch et al., 1995; Rodgers and Rowland, 2007
Diazepam	N	0.012 (9%)	0.74 (4%)	2.82	14	3.4	0.64	1.79	1.33	Maguire et al., 1980; Sangster, 1993; O'Neil, 2006
Felodipine	N	0.0017 (12%)	0.023 (27%)	3.86	14	5.07	0.7	2.95	41.7	Diez et al., 1991; Uchimura et al., 2010; Pandey et al., 2013
Fluconazole	N	0.93 (14%)	0.94 (14%)	0.8	14	1.77	1	−0.79	1.25	Debruyne et al., 1987; Debruyne, 1997; Rodgers and Rowland, 2007
Midazolam	N	0.033 (4%)	0.71 (4%)	3.15	14	6.01	0.53	2.16	18	Heizmann et al., 1983; Rodgers and Rowland, 2007
Phenytoin	N	0.18 (7%)	0.83 (3%)	2.21	8.32	1	0.61	1.11	1.61	Stella et al., 1998; Brittain, 2007; Uchimura et al., 2010
Diclofenac	A	0.0014 (18%)	0.78 (4%)	4.51	4.15	1	0.55	3.68	17.6	Sangster, 1994; Obach, 1999; Avdeef, 2003
Glyburide	A	0.0012 (16%)	0.72 (9%)	4.29	5.38	1	0.57	2.59	4.81	Austin et al., 2002; Li et al., 2017
Ketoprofen	A	0.0041 (9%)	0.95 (4%)	3.12	4.45	1	0.56	2.06	5.02	Sangster, 1993, 1994; Rodgers and Rowland, 2007; Ye et al., 2016
Nafcillin	A	0.123 (6%)	0.94 (14%)	2.7	2.6	1	0.55[d]	1.66	33.9	Wishart et al., 2018
Warfarin	A	0.0076 (13%)	0.98 (16%)	2.7	5.05	1	0.55	1.66	0.179	Hiskey et al., 1962; Hansch et al., 1995; Obach, 1999

A, acids; B, bases; N, neutral; CL, clearance; vo, vegetable oil.
[a]All 98 experimental values unless otherwise noted.
[b]Rat BP was used.
[c]An average of literature values was used.
[d]0.55 was used (1-hematocrit).

the fraction unbound in matrix measured during the assay. The average fraction unbound, S.D., and CV values were determined for each assay.

Simulations. A generic PBPK model was used, with different tissues represented by 10 compartments (adipose, bone, brain, gut, kidney, liver, lungs, muscle, skin, and spleen), representing the major tissues in the body (Fig. 1). These compartments are linked via arterial and venous blood flows. The K_p values were predicted for each of the tissues using both methods ($K_{p,dPL}$ and $K_{p,mem}$). The original $K_{p,dPL}$ method uses two separate equations, one for acids, weak bases, and neutrals, and another for moderate-to-strong bases (eqs. 4–7) (Rodgers et al., 2005; Rodgers and Rowland, 2006).

The $K_{p,dPL}$ equation used for prediction of K_{pu} for strong-to-moderate bases is

$$K_{pu,tissue} = f_{ew} + \frac{1 + 10^{pK_{a,b} - pH_{iw}}}{1 + 10^{pK_{a,b} - pH_p}} \cdot f_{iw} + \frac{K_{AP} \cdot [AP] \cdot 10^{pK_{a,b} - pH_{iw}}}{1 + 10^{pK_{a,b} - pH_{iw}}} + P \cdot f_{nl} + \frac{(0.3P + 0.7) \cdot f_{npl}}{1 + 10^{pK_{a,b} - pH_p}} \quad (4)$$

where f_{ew} is the fractional volume of extracellular water; f_{iw} is the fractional volume of intracellular water; [AP] is the concentration of acidic phospholipids in the tissue; K_{AP} is the association constant for acidic phospholipids in the tissue; f_{nl} is the fractional volume of neutral lipids; f_{npl} is the fractional volume of neutral phospholipids; $pK_{a,b}$ is the basic ionization constant; and $pK_{a,a}$ is the acidic ionization constant.

The Rodgers equation used for prediction of K_{pu} for acids, neutrals, and weak bases is

$$K_{pu,tissue} = f_{ew} + \frac{1 + 10^{pH_{iw} - pK_{a,a}}}{1 + 10^{pH_p - pK_{a,a}}} \cdot f_{iw} + \frac{P \cdot f_{nl} + (0.3P + 0.7) \cdot f_{NP}}{1 + 10^{pH_p - pK_{a,a}}} + \left[\frac{1}{f_{up}} - 1 - \left(\frac{P \cdot f_{nl} + (0.3P + 0.7) \cdot f_{NP}}{1 + 10^{pH_p - pK_{a,a}}}\right)\right] \cdot \frac{[PR]_T}{[PR]_P} \quad (5)$$

where $[PR]_T/[PR]_P$ is the plasma protein tissue (extracellular fluid) to plasma ratio, and NP denotes neutral phospholipid.

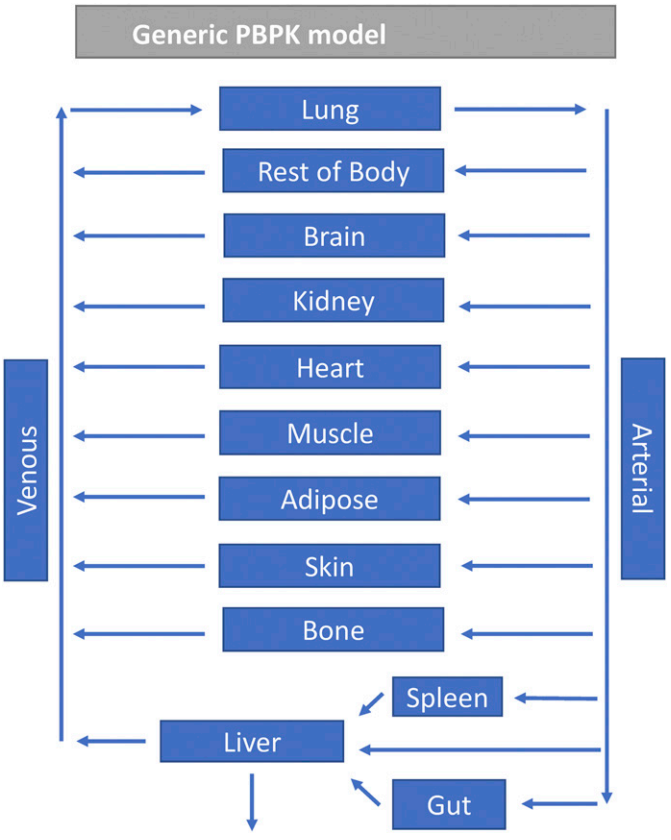

Fig. 1. Scheme for the generic PBPK model used in this study.

For eq. 4, the association constant for blood cells (BCs) is defined in eq. 6, and the tissue:plasma water partitioning coefficient for the BCs is defined in eq. 7:

$$K_{a,BC} = \left(K_{pu,BC} - \frac{1 + 10^{pK_a - pH_{BC}}}{1 + 10^{pK_a - pH_p}} f_{iw,BC} - \frac{P_{ow} \cdot f_{nl,BC} + (0.3P_{ow} + 0.7) f_{np,BC}}{1 + 10^{pK_a - pH_p}}\right) \cdot \left(\frac{1 + 10^{pK_a - pH_p}}{[AP^-]_{BC} 10^{pK_a - pH_{BC}}}\right) \quad (6)$$

$$K_{pu,BC} = \frac{BP + H - 1}{H \cdot f_{up}} \quad (7)$$

The tissue:plasma partition coefficient (K_p) can be determined from K_{pu} by eq. 8:

$$K_p = K_{pu} \cdot f_{up} \quad (8)$$

For the $K_{p,mem}$ method we use the previously reported equation (Korzekwa and Nagar, 2017a) that considers both phospholipid membrane partitioning with f_{um} and neutral lipid partitioning with P (eq. 9):

$$K_{p,tissue} = r(1 - f_{up}) + f_{iw} \cdot f_{up} \cdot \frac{10^{pK_{a,b} - 7.0} + 10^{7.0 - pK_{a,a}} + 1}{10^{pK_{a,b} - 7.4} + 10^{7.4 - pK_{a,a}} + 1} + f_{ew} \cdot f_{up} + f_{pl} \cdot \frac{10^{pK_{a,b} - 7.0} + 10^{7.0 - pK_{a,a}} + 1}{10^{pK_{a,b} - 7.4} + 10^{7.4 - pK_{a,a}} + 1} \cdot f_{up} \cdot a \cdot LKL + \frac{f_{nl} \cdot f_{up} \cdot b \cdot P}{10^{pK_{a,b} - 7.0} + 10^{7.0 - pK_{a,a}} + 1} \quad (9)$$

where r is the protein ratio between the tissue and plasma; f_{pl} is the fractional volume of phospholipid; LKL is the lipid binding constant; and a and b are parameterized coefficients. Plasma and tissue pH values were assumed to be 7.4 and 7.0, respectively. As described previously for V_{ss} predictions (Korzekwa and Nagar, 2017a), the tissue-specific r values for bases were decreased by 2.23-fold due to the lower amount of α-acid glycoprotein in the extracellular fluid relative to albumin (Rowland and Tozer, 2011).

Neutral lipid partitioning in adipose tissue is described by the vegetable oil:water partition coefficient in the $K_{p,dPL}$ method, which is generally calculated from log P. In the $K_{p,mem}$ prediction method log P is used directly. The a and b terms in eq. 9 were parameterized using the tissue K_p values and tissue composition data from Rodgers et al. (2005) and Rodgers and Rowland (2006). We excluded zwitterions and combined neutral and acidic phospholipids to obtain a fraction of the total phospholipids. Most f_{um} values were calculated with our previously reported model (Nagar and Korzekwa, 2017) since experimental values are not available for this data set. The log K_{pu} values and the log of eq. 9 were used to fit a and b, with no additional weighting (log transformation results in $1/Y$ weighting). Outliers were identified using the BoxWhisker function (Frigge et al., 1989) in Mathematica with outliers defined as >1.5 times the interquartile range. Another model, which included an additional parameter for partitioning into adipose, was evaluated but did not improve predictions. The lipid concentrations multiplied by the lipid binding constant, L times K_L, (LKL), was calculated from f_{um} with eq. 10, using f_{um} values normalized to 1 mg/ml microsomal protein:

$$LKL = L \times K_L = \frac{1 - f_{um}}{f_{um}} \quad (10)$$

Exposure overlap coefficients (EOCs) were used to quantify the ability to predict the shape of the C-t profile (eq. 11) (Nagar et al., 2017). They are calculated by determining the overlapping portion of the experimental and predicted C-t profile curves and dividing that area by the experimental area under the curve (AUC). Since the experimental clearance values were used for all predictions, both experimental and predicted C-t profiles will have the same AUC. This allows the EOC to be used as a direct comparison of curve shapes. Differences in the average EOCs were determined using the t test:

$$EOC = \frac{\text{Overlapping area}}{AUC} \quad (11)$$

***V_{ss}* Predictions.** The V_{ss} value was determined from the predicted K_p values and physiologic volumes (eq. 12):

$$V_{ss} = V_p + \sum V_t \cdot K_p \quad (12)$$

where V_p is the plasma volume, and V_t represents the tissue volume.

Predicted V_{ss} values were compared with observed values determined by compartmental modeling. To evaluate the predictive precision of the two methods, the absolute fold-error and absolute average fold error (AAFE) values were determined for all compounds and different subsets. Significance of differences in absolute fold errors were determined with a one-tailed t test. The AAFE determines the geometric mean of the absolute fold error (eq. 13) and is a measure of how precisely the two methods predict V_{ss}:

$$\text{AAFE} = 10^{(1/n)\sum \log FE} \quad (13)$$

where n is the number of drugs, and FE is the fold error.

Results

The parameters a and b in eq. 9 were fit to the experimental tissue reported K_{pu} values for the rat (Rodgers et al., 2005; Rodgers and Rowland, 2006). After sequential removal of 20 outliers (out of 401), the optimized parameters were a = 1383 ± 85 and b = 0.096 ± 0.029. The predicted versus observed K_{pu} values for 381 drugs are shown in Fig. 2. The R^2 value for the fit was 0.80. There was no consistent characteristic for the removed outliers with the exception of the overprediction of phencyclidine in four tissues and the underprediction of basic compounds in the lung (five drugs).

Figure 3 and Table 3 show the observed versus predicted V_{ss} values using either the $K_{p,dPL}$ or $K_{p,mem}$ prediction method. The accuracy of the V_{ss} predictions was analyzed by determining the percentage of predictions within a range of absolute fold errors (Table 4) and AAFEs (Table 5). For the total data set of 19 drugs, the $K_{p,mem}$ and $K_{p,dPL}$ methods had comparable AAFE values (2.12 and 2.27, respectively). The $K_{p,mem}$ and $K_{p,dPL}$ methods had one (mibefradil) and two (diphenhydramine, felodipine) outliers, respectively. When these were excluded, the AAFEs were again comparable.

Ten different categories are compared in Tables 4 and 5. For predictions that were less than 1.5-fold error, $K_{p,mem}$ scored higher in five categories, lower in two categories, and the same in three categories compared with $K_{p,dPL}$ (Table 4); for predictions that were less than 3-fold error, $K_{p,mem}$ scored lower in five categories and the same in five categories compared with $K_{p,dPL}$. When comparing all 19 drugs, the AAFEs with $K_{p,mem}$ versus $K_{p,dPL}$ were 2.12 versus 2.27, respectively (Table 5). Across the 10 categories, the AAFE was lower for $K_{p,mem}$ than for $K_{p,dPL}$ in eight categories. When outliers were excluded in each method, the AAFE was lower for $K_{p,mem}$ than for $K_{p,dPL}$ in five categories. For all categories listed in Table 5, there were no statistically significant differences in average fold error between $K_{p,mem}$ and $K_{p,dPL}$.

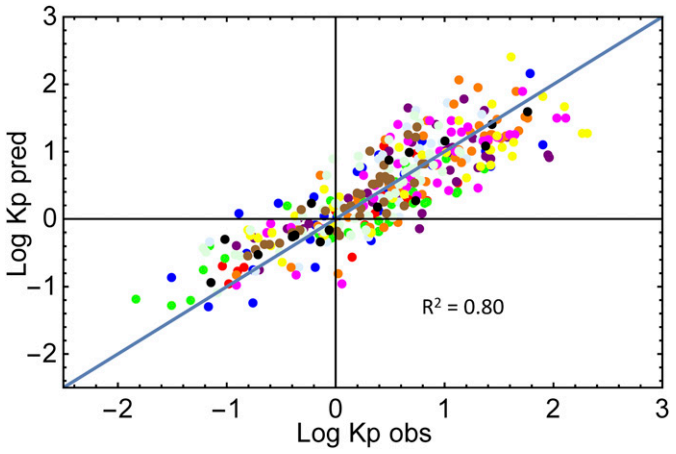

Fig. 2. Observed vs. predicted rat K_{pu} values from eq. 10: blue, adipose; red, bone; green, brain; purple, gut; light blue, heart; orange, kidney; magenta, liver; yellow, lung; light green, muscle; brown, skin; black, spleen.

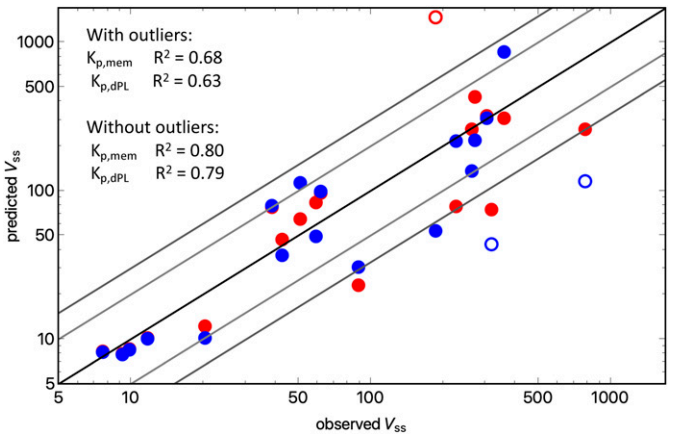

Fig. 3. Observed V_{ss} value vs. predicted V_{ss} value for 19 drugs: blue, $K_{p,dPL}$; red, $K_{p,mem}$.

Simulations. An example of EOC calculation is shown in Fig. 4 for verapamil. Concentration profiles were simulated for 19 drugs with both K_p prediction methods (Figs. 5–7). EOCs were determined for all 19 drugs (Table 3). Overall, there was no significant difference in the average EOC values for the $K_{p,mem}$ or $K_{p,dPL}$ method. However, there were some interesting deviations between the methods. The C-t profiles were poorly predicted by both methods for five drugs: mibefradil, diazepam, felodipine, diclofenac, and nafcillin. In addition, the $K_{p,dPL}$ method poorly predicted the profiles for betaxolol and diphenhydramine. Some possible explanations for these discrepancies are discussed subsequently.

As discussed previously (Korzekwa and Nagar, 2017b), eqs. 5–7 indicate that the $K_{pu,tissue}$ value, and ultimately the unbound V_{ss} value, should be proportional to $K_{pu,BC}$ (eq. 7), which was first experimentally observed by Hinderling (1997). Also, f_{up} in the denominator of eq. 7 is ultimately multiplied by f_{up} in the PBPK framework (eq. 8). Therefore, the predicted V_{ss} values for bases should be relatively insensitive to f_{up} when using eqs. 4–7. The impact on the predicted V_{ss} after a 2-fold decrease in f_{up} is shown in Table 6. As expected, changing f_{up} for acids has little effect since plasma protein binding is high and V_{ss} is low. For neutrals, a 2-fold decrease in f_{up} results in an average 1.7-fold increase in V_{ss} for both methods. For bases, a 2-fold decrease in f_{up} results in an average 2-fold decrease in V_{ss} for $K_{p,mem}$, but an average 1.05-fold increase with $K_{p,dPL}$.

Discussion

Tissue partition coefficients, and ultimately V_{ss}, are determined primarily by competition between plasma protein binding and lipid partitioning. The $K_{p,dPL}$ method considers binding to neutral lipids such as triglycerides and neutral phospholipids in membranes, with acidic phospholipids considered separately (Rodgers et al., 2005; Rodgers and Rowland, 2006). The method assumes that neutral molecules only interact with neutral phospholipids, and only ionized bases interact with APs, an assumption questioned previously (Korzekwa and Nagar, 2017b). The major acidic phospholipid is phosphatidylserine and the major neutral phospholipid is phosphatidylcholine. Although phosphatidylcholine is net neutral and phosphatidylserine is net acidic, both molecules are zwitterions. Interactions between charged species in the polar head group region are dynamic processes with conformational changes occurring in a picosecond time frame (Tieleman et al., 1997).

TABLE 3

Observed and predicted V_{ss} and EOC values for both methods

Test Drug	Observed V_{ss}	Predicted V_{ss}		EOC	
		$K_{p,mem}$ Method	$K_{p,dPL}$ Method	$K_{p,mem}$ Method	$K_{p,dPL}$ Method
	l	*l*	*l*		
Betaxolol	360	307	856	0.97	0.61
Diltiazem	306	320	309	0.76	0.80
Diphenhydramine	788	260	115	0.97	0.87
Metoprolol	274	429	217	0.76	0.87
Mibefradil	187	1470	53.2	0.81	0.82
Nicardipine	62	96.4	98.5	0.79	0.78
Quinidine	227	78.3	215	0.96	0.73
Verapamil	266	258	136	0.73	0.76
Caffeine	42.8	47.0	36.7	0.87	0.93
Diazepam	89.5	22.9	30.5	0.55	0.61
Felodipine	320	74.3	43.4	0.68	0.56
Fluconazole	59.3	83.4	49.1	0.85	0.99
Midazolam	51.2	64.1	113	0.82	0.71
Phenytoin	38.8	77.0	79.1	0.78	0.77
Diclofenac	9.23	7.98	7.89	0.84	0.84
Glyburide	11.78	10.2	10.0	0.86	0.87
Ketoprofen	9.9	8.54	8.47	0.89	0.89
Nafcillin	20.4	12.2	10.1	0.86	0.81
Warfarin	7.66	8.20	8.15	0.96	0.97
			Average	0.82 ± 0.11	0.80 ± 0.12

Balaz (2009) compiled experimental data evaluating the orientation of exogenous molecules in membranes. Hydrophilic molecules accumulate in the polar head group region, amphiphilic molecules accumulate at the interface, and hydrophobic molecules accumulate in the hydrophobic core. We have used this concept to develop quantitative models for membrane partitioning (Nagar and Korzekwa, 2017).

The $K_{p,mem}$ model is based on previously reported V_{ss} models (Korzekwa and Nagar, 2017a). The K_p model described herein uses the phospholipid component of tissues and f_{um} to model membrane partitioning and log *P* for neutral lipid interactions. Equation 9 was parameterized using reported tissue composition data and tissue K_p values (Rodgers et al., 2005; Rodgers and Rowland, 2006). Only two constants were parameterized: the scaling factor for 1) membranes and 2) neutral lipids. Although the two methods use different mechanistic assumptions, the resulting fit for $K_{p,mem}$ (Fig. 2) is similar to that reported by Rodgers et al. (2005) for K_{pu} parameterization.

The volume of distribution is generally low for acids due to high plasma protein binding and low partitioning into membranes and neutral lipids. At physiologic pH, most acids are negatively charged, and membranes have few hydrogen bond donors. Therefore, microsomal partitioning is low for acids, with f_{um} values ranging from 0.72 to 0.98 (Table 2). Both the $K_{p,mem}$ and $K_{p,dPL}$ methods assume that only the neutral acids partitions into tissues, and both methods predict V_{ss} with similar accuracy (AAFE = 2.12 and 2.27 for $K_{p,mem}$ and $K_{p,dPL}$, respectively) (Table 5). This is expected since any model that restricts a compound with low f_{up} to the plasma and extracellular space will predict a V_{ss} value approximately equal to that of plasma proteins (~7.5 l) (Rowland and Tozer, 2011). Underprediction of acids with V_{ss} values >9, e.g., nafcillin, is frequently observed (Chan et al., 2018). Transporter activity (e.g., organic anion transporting polypeptides) could be one reason for the underprediction.

When two outliers for the $K_{p,dPL}$ analysis (diphenhydramine and felodipine) are excluded, V_{ss} predictions for neutrals using $K_{p,dPL}$ improved from an AAFE value of 2.82 to 1.91 (Table 5). For diphenhydramine, the $K_{p,dPL}$ method resulted in a 6.9-fold underprediction and $K_{p,mem}$ gave a 3-fold underprediction (not an outlier). For felodipine, $K_{p,dPL}$ resulted in a 7.4-fold underprediction and $K_{p,mem}$ gave a 4.3-fold underprediction (not an outlier). The reason for these poor predictions is unknown but it may be difficult to predict V_{ss} of a highly protein bound and partitioned neutral compound (felodipine).

The $K_{p,mem}$ method uses a single equation for bases, neutrals, and acids and predicts V_{ss} for bases with similar accuracy to $K_{p,dPL}$, which uses different equations for bases (eqs. 5–7). The $K_{p,dPL}$ method assumes that ionized bases only interact with acidic phospholipids. This interaction

TABLE 4

Fraction of drugs in which the predictions had less than 1.5-, 2-, and 3-fold error

Category	<1.5-Fold Error		<2-Fold Error		<3-Fold Error	
	$K_{p,mem}$	$K_{p,dPL}$	$K_{p,mem}$	$K_{p,dPL}$	$K_{p,mem}$	$K_{p,dPL}$
All Compounds	10/19	9/19	14/19	11/19	15/19	16/19
Acids	4/5	4/5	5/5	4/5	5/5	5/5
Bases	3/8	3/8	5/8	5/8	6/8	6/8
Neutrals	3/6	2/6	4/6	2/6	4/6	5/6
Log P <3	5/9	5/9	8/9	5/9	8/9	9/9
Log P >3	5/10	4/10	6/10	6/10	7/10	7/10
$f_{um} < 0.8$	6/11	4/11	8/11	6/11	8/11	9/11
$f_{um} > 0.8$	4/8	5/8	6/8	5/8	7/8	7/8
$f_{up} < 0.1$	6/10	4/10	7/10	6/10	7/10	8/10
$f_{up} > 0.1$	4/9	5/9	7/9	8/9	8/9	8/9

TABLE 5

Absolute average fold error for V_{ss} predictions using both the $K_{p,mem}$ and $K_{p,dPL}$ prediction methods

Category	AAFE		AAFE (Excluding Outliers)	
	$K_{p,mem}$	$K_{p,dPL}$	$K_{p,mem}$	$K_{p,dPL}$
All Compounds	2.12	2.27	1.80	1.70
Acids	1.24	1.32	1.24	1.32
Bases	2.52	2.45	1.76	1.82
Neutrals	2.32	2.82	2.32	1.91
Log P <3	1.66	1.68	1.66	1.68
Log P >3	2.54	2.81	1.95	1.73
f_{um} < 80%	2.36	2.41	1.81	1.92
f_{um} > 80%	1.79	2.07	1.79	1.39
f_{up} < 10%	2.45	2.42	1.84	1.86
f_{up} > 10%	1.76	2.11	1.76	1.56

is parameterized with BP, using the erythrocyte partition coefficient to parameterize binding of the ionized base to acidic phospholipids. Mechanistically, the assumption that bases bind only to acidic phospholipids is questionable. Hydrophobic bases bind to neutral phospholipids as well, with key interactions between the cation and negatively charged phosphate, and the hydrophobic region with the hydrophobic membrane core. From eqs. 5–7, it is clear that for moderate-to-strong bases with V_{ss} values greater than the total body water, the K_p values are dominated by the acidic phospholipid binding terms. Therefore, although binding to only acidic phospholipids was assumed, a similar relationship is possible, assuming that ionized bases bind to all phospholipids. The ratio of neutral to acidic phospholipids is relatively constant across tissues (CV = 15%) (Rodgers et al., 2005), and total phospholipids can be substituted for neutral phospholipids. The K_{BC} term in eq. 6 would be smaller, but the relevant phospholipid term in eq. 5 would be larger.

Another implication of using BP to predict K_{pu} for bases is the insensitivity of V_{ss} to measured f_{up}. For acids, V_{ss} is insensitive to f_{up} since tissue partitioning is minimal. The V_{ss} values for bases are expected to be proportional to f_{up} since they partition heavily into tissues from the unbound concentration in cytosol (assumed to be equal to the unbound concentration in plasma). This is observed for $K_{p,mem}$ but not for $K_{p,dPL}$ (Table 6). This is a consequence of using BP (which includes f_{up}) to calculate K_{pu}. The V_{ss} predictions can be relatively accurate when BP is used to predict K_p for bases, since errors in f_{up} are not manifest and unbound V_{ss} for bases is proportional to erythrocyte partitioning (Hinderling, 1997). However, errors in f_{up} can still result in many other inaccuracies, including in predictions of clearance and target activity.

Overall, the $K_{p,mem}$ and $K_{p,dPL}$ models give similarly accurate predictions, explaining 68% and 63% of the variance in V_{ss} (80% and 79% without outliers), respectively. Several factors may explain the remaining variance. First, there can be significant variability in the V_{ss} values measured across clinical studies. Not all pharmacokinetic data sets provide body weights. Also, experimental data from multiple sources are used, e.g., BP values; for example, Graham et al. (2012) observed a 7% decrease in accuracy when predicted instead of experimental log P values were used. For f_{up}, differences between laboratories can be very large. Several recent publications discuss assay conditions for protein binding, including dilution and use of CO_2 (Kochansky et al., 2008; Curran et al., 2011; Di et al., 2017). In this study, we measured a value of f_{up} of 0.03 for mibefradil, whereas a value of <0.005 was reported previously (Clozel et al., 1991). Use of a smaller f_{up} value would result in a better prediction with $K_{p,mem}$, but exclusion of our data is not justified.

Lysosomal partitioning affects tissue distribution for bases. For strong bases, partitioning into lysosomes due to pH differences results in lysosomal concentrations >200 times cytosolic concentrations. Assuming 5% lysosomes and 60% intracellular water in cells, partitioning of a strong base into lysosomes can increase the K_{pu} value by 6-fold. As discussed previously, while lysosomal partitioning certainly occurs it is likely to be highly correlated with phospholipid partitioning of bases (Korzekwa and Nagar, 2017a). Finally, although the vegetable oil:water partition constant would be a good surrogate for adiposomes if measured, this value is typically modeled using log P, which is not necessarily accurate (Korzekwa and Nagar, 2017b).

Transporter-mediated distribution can result in inaccurate predictions of K_p and V_{ss}, particularly for some acids. Organic anion transporting polypeptide transporters can alter hepatic intracellular concentrations by two orders of magnitude (Kulkarni et al., 2016). Therefore, uptake into this organ alone can result in a 2-fold increase in V_{ss}. Efflux transporters

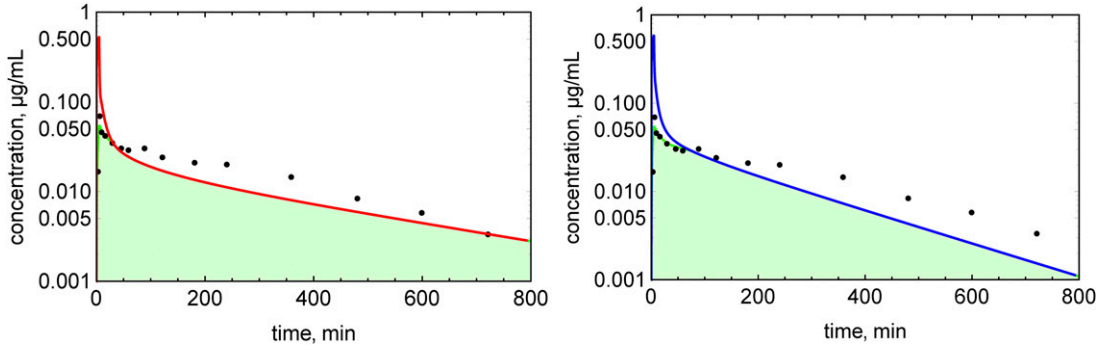

Fig. 4. Determination of the exposure overlap coefficients for verapamil: red line, simulated C-t profile using the $K_{p,mem}$ method; blue line, simulated C-t profile using the $K_{p,dPl}$ method; green area, area of overlap.

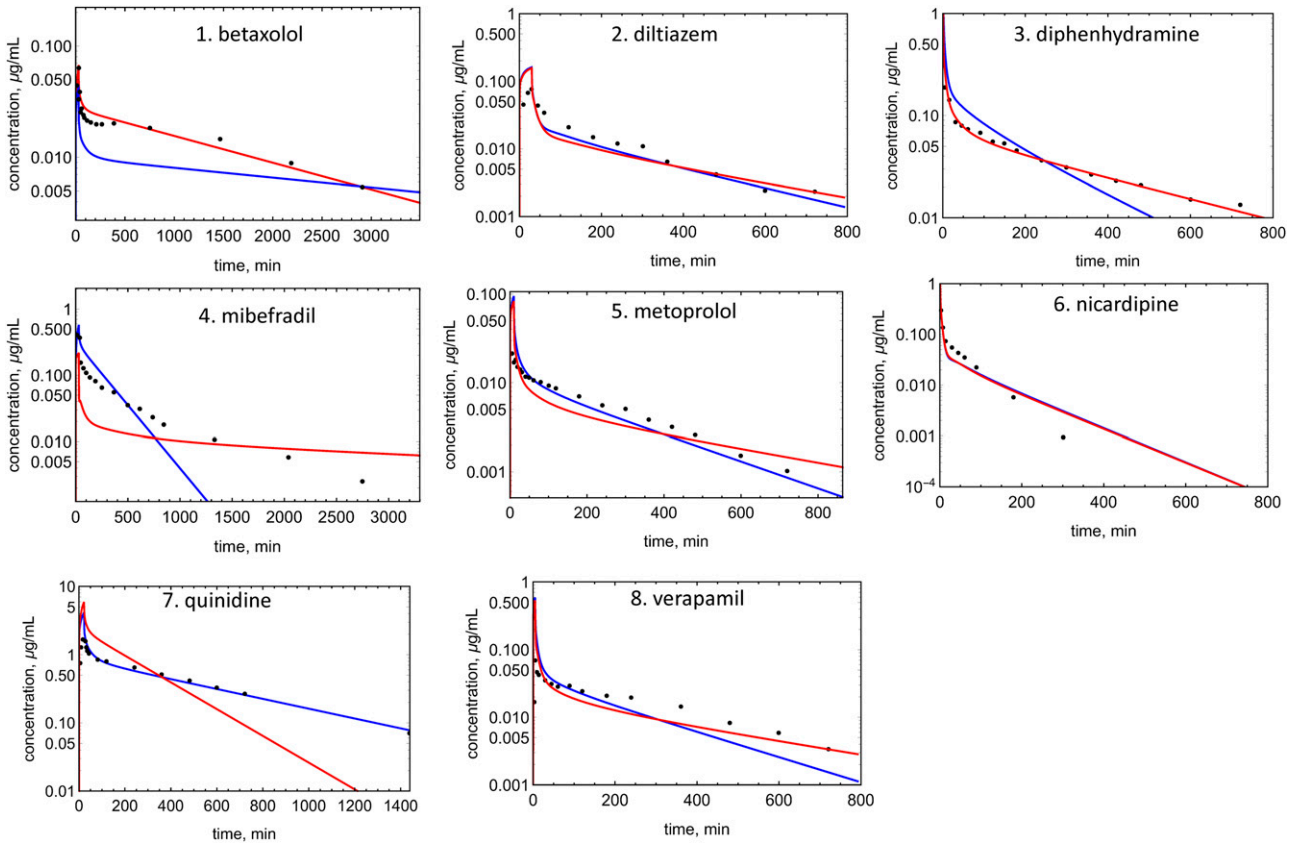

Fig. 5. Observed and predicted C-t profiles for bases: red lines, simulated C-t profile using the $K_{p,mem}$ method; blue lines, simulated C-t profile using the $K_{p,dPl}$ method; solid circles, experimental data.

(e.g., P-glycoprotein and breast cancer resistance protein) will have a smaller impact. The decrease in V_{ss} due to P-glycoprotein and breast cancer resistance protein at the blood-brain barrier would result in a 2% decrease in V_{ss}. The impact from the liver would be even smaller since efflux transporters in the apical membrane would only decrease liver concentrations by 50% (Korzekwa and Nagar, 2014).

Since the AUC is determined by experimental clearance and dose in both methods, the AUC values for the simulations are normalized, and the EOC captures differences in the shapes of the C-t profile (Fig. 4). Several C-t profiles in Figs. 5–7 are not well predicted by either method. Although there are differences in the EOC for some drugs, the average EOCs for the $K_{p,mem}$ and $K_{p,dPL}$ prediction methods were not

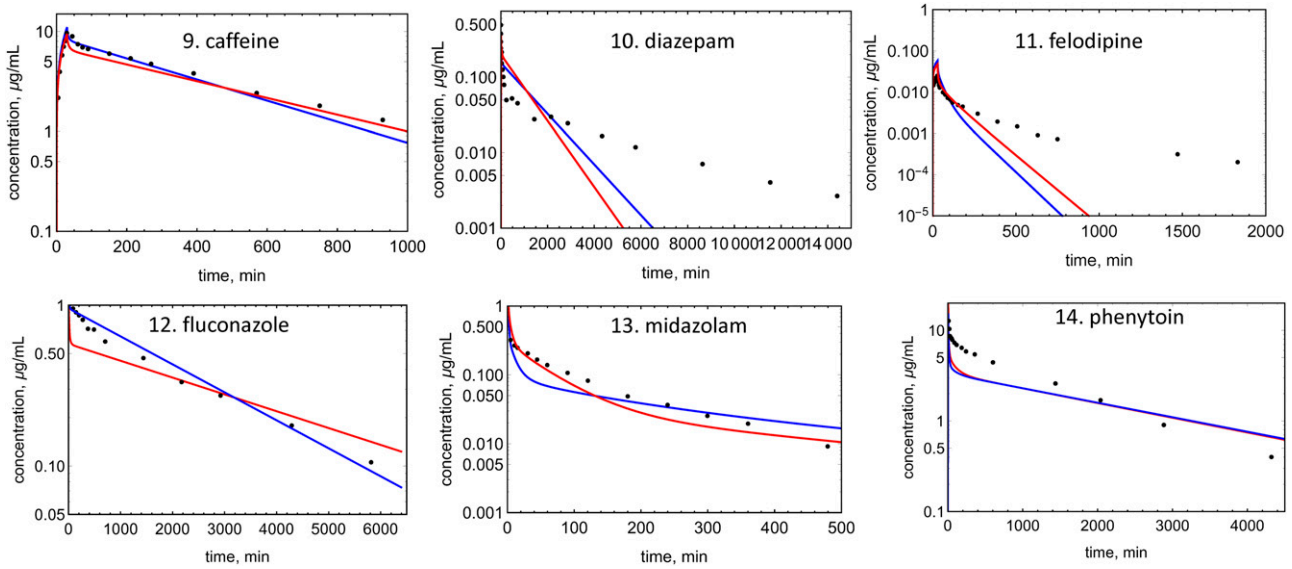

Fig. 6. Observed and predicted C-t profiles for neutral molecules: red lines, simulated C-t profile using the $K_{p,mem}$ method; blue lines, simulated C-t profile using the $K_{p,dPl}$ method; solid circles, experimental data.

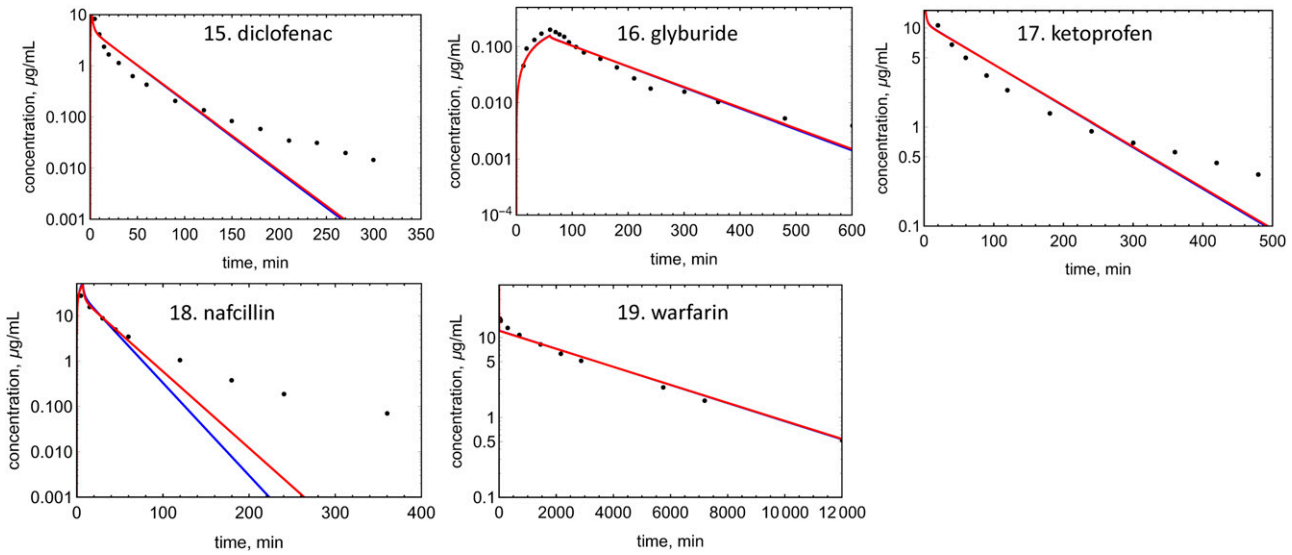

Fig. 7. Observed and predicted C-t profiles for acids: red lines, simulated C-t profile using the $K_{p,mem}$ method; blue line, simulated C-t profile using the $K_{p,dPl}$ method; solid circles, experimental data.

significantly different. Since clearance is constant, when the V_{ss} value is overpredicted (e.g., betaxolol using $K_{p,dPL}$ and mibefradil using $K_{p,mem}$) (Fig. 5), the terminal half-life is overpredicted. When the V_{ss} value is underpredicted (e.g., diphenhydramine using $K_{p,dPL}$) (Fig. 5), the terminal half-life is underpredicted. Perhaps the most significant deficiency of the reported modeling approaches is the assumption of perfusion-limited distribution. As seen with diazepam, felodipine, diclofenac, and nafcillin, accurate C-t profiles are not predicted even when the V_{ss} value is well predicted. For verapamil (Figs. 4 and 5), the distribution phase is not well predicted, presumably due to a combination of using a perfusion-limited model and experimental clearance. Clearly, multicompartmental distribution is not accurately modeled with perfusion-limited distribution.

In conclusion, $K_{p,mem}$ can be used to predict K_{pu} with accuracy similar to $K_{p,dPL}$. An advantage of using f_{um} to parameterize membrane partitioning is that f_{um} is used for clearance prediction and is generated early in the discovery/development process. Also, differentiating between acidic and neutral phospholipids for bases and using 0.3*P* for neutral compounds is not mechanistically justified. Finally, since both the extent and rate of membrane partitioning and permeability are important, a mechanistically sound basis for membrane interactions is necessary for improved PBPK models.

TABLE 6

Impact of errors in f_{up} on V_{ss}

Compound	Fold Decrease in V_{ss} upon a 2-Fold Decrease in f_{up}	
	$K_{p,mem}$	$K_{p,dPL}$
Betaxolol	1.97	0.95
Diltiazem	1.98	1.05
Diphenhydramine	1.94	0.82
Metoprolol	1.98	0.75
Mibefradil	2.00	0.95
Nicardipine	1.90	1.01
Quinidine	1.89 [average (bases)]	1.00 [average (bases)]
Verapamil	1.95 (1.95 ± 0.04)	1.06 (0.95 ± 0.11)
Caffeine	1.66	1.59
Diazepam	1.41	1.53
Felodipine	1.79	1.66
Fluconazole	1.82	1.70
Midazolam	1.78 [average (neutrals)]	1.86 [average (neutrals)]
Phenytoin	1.78 (1.71 ± 0.15)	1.79 (1.69 ± 0.12)
Diclofenac	1.01	1.01
Glyburide	1.05	1.03
Ketoprofen	1.01	1.00
Nafcillin	1.19 [average (acids)]	1.09 [average (acids)]
Warfarin	1.01 (1.05 ± 0.08)	1.01 (1.03 ± 0.04)

Authorship Contributions

Participated in research design: Holt, Nagar, Korzekwa.

Conducted experiments: Holt, Ye.

Performed data analysis: Holt, Nagar, Korzekwa.

Wrote or contributed to the writing of the manuscript: Holt, Nagar, Korzekwa.

References

Agarwal SK, Kriel RL, Brundage RC, Ivaturi VD, and Cloyd JC (2013) A pilot study assessing the bioavailability and pharmacokinetics of diazepam after intranasal and intravenous administration in healthy volunteers. *Epilepsy Res* **105**:362–367.

Akaike T (1974) A new look at the statistical model identification. *IEEE Trans Autom Control* **19**: 716–723.

Albert KS, Hallmark MR, Sakmar E, Weidler DJ, and Wagner JG (1975) Pharmacokinetics of diphenhydramine in man. *J Pharmacokinet Biopharm* **3**:159–170.

Arundel P (1997) A multi-compartmental model generally applicable to physiologically-based pharmacokinetics. *IFAC Proc Vol*, **30**:129–133.

Austin RP, Barton P, Cockroft SL, Wenlock MC, and Riley RJ (2002) The influence of nonspecific microsomal binding on apparent intrinsic clearance, and its prediction from physicochemical properties. *Drug Metab Dispos* **30**:1497–1503.

Avdeef A (2003) *Absorption and Drug Development: Solubility, Permeability, and Charge State*, Wiley, Hoboken, NJ.

Balaz S (2009) Modeling kinetics of subcellular disposition of chemicals. *Chem Rev* **109**: 1793–1899.

Berezhkovskiy LM (2004) Volume of distribution at steady state for a linear pharmacokinetic system with peripheral elimination. *J Pharm Sci* **93**:1628–1640.

Björkman S (2002) Prediction of the volume of distribution of a drug: which tissue-plasma partition coefficients are needed? *J Pharm Pharmacol* **54**:1237–1245.

Blanchard J and Sawers SJA (1983) The absolute bioavailability of caffeine in man. *Eur J Clin Pharmacol* **24**:93–98.

Brittain H (2007) *Profiles of Drug Substances, Excipients, and Related Methodology*, Academic Press, Cambridge, MA.

Brown RP, Delp MD, Lindstedt SL, Rhomberg LR, and Beliles RP (1997) Physiological parameter values for physiologically based pharmacokinetic models. *Toxicol Ind Health* **13**: 407–484.

Campbell BC, Kelman AW, and Hillis WS (1985) Noninvasive assessment of the haemodynamic effects of nicardipine in normotensive subjects. *Br J Clin Pharmacol* **20** (Suppl 1): 55S–61S.

Chan R, De Bruyn T, Wright M, and Broccatelli F (2018) Comparing mechanistic and preclinical predictions of volume of distribution on a large set of drugs. *Pharm Res* **35**:87.

Clozel JP, Osterrieder W, Kleinbloesem CH, Welker HA, Schlappi B, Tudor R, Hefti F, Schmitt R, and Eggers H (1991) RO 40-5967: a new nonhydropyridine calcium antagonist. *Cardiovasc Drug Rev* **9**:4–17.

Curran RE, Claxton CRJ, Hutchison L, Harradine PJ, Martin IJ, and Littlewood P (2011) Control and measurement of plasma pH in equilibrium dialysis: influence on drug plasma protein binding. *Drug Metab Dispos* **39**:551–557.

De Buck SS, Sinha VK, Fenu LA, Gilissen RA, Mackie CE, and Nijsen MJ (2007) The prediction of drug metabolism, tissue distribution, and bioavailability of 50 structurally diverse compounds in rat using mechanism-based absorption, distribution, and metabolism prediction tools. *Drug Metab Dispos* **35**:649–659.

Debruyne D (1997) Clinical pharmacokinetics of fluconazole in superficial and systemic mycoses. *Clin Pharmacokinet* **33**:52–77.

Debruyne D, Hurault de Ligny B, Ryckelynck JP, Albessard F, and Moulin M (1987) Clinical pharmacokinetics of ketoprofen after single intravenous administration as a bolus or infusion. *Clin Pharmacokinet* **12**:214–221.

Di L, Breen C, Chambers R, Eckley ST, Fricke R, Ghosh A, Harradine P, Kalvass JC, Ho S, Lee CA, et al. (2017) Industry perspective on contemporary protein-binding methodologies: considerations for regulatory drug-drug interaction and related guidelines on highly bound drugs. *J Pharm Sci* **106**:3442–3452.

Diez I, Colom H, Moreno J, Obach R, Peraire C, and Domenech J (1991) A comparative in vitro study of transdermal absorption of a series of calcium channel antagonists. *J Pharm Sci* **80**:931–934.

Edgar B, Regårdh CG, Johnsson G, Johansson L, Lundborg P, Löfberg I, and Rönn O (1985) Felodipine kinetics in healthy men. *Clin Pharmacol Ther* **38**:205–211.

Fenneteau F, Poulin P, and Nekka F (2010) Physiologically based predictions of the impact of inhibition of intestinal and hepatic metabolism on human pharmacokinetics of CYP3A substrates. *J Pharm Sci* **99**:486–514.

Frigge M, Hoaglin DC, and Iglewicz B (1989) Some implementations of the boxplot. *Am Statistician* **43**:50–54.

Ghafourian T, Barzegar-Jalali M, Hakimiha N, and Cronin MTD (2004) Quantitative structure-pharmacokinetic relationship modelling: apparent volume of distribution. *J Pharm Pharmacol* **56**:339–350.

Graham H, Walker M, Jones O, Yates J, Galetin A, and Aarons L (2012) Comparison of in-vivo and in-silico methods used for prediction of tissue: plasma partition coefficients in rat. *J Pharm Pharmacol* **64**:383–396.

Greene DS, Quintiliani R, and Nightingale CH (1978) Physiological perfusion model for cephalosporin antibiotics I: model selection based on blood drug concentrations. *J Pharm Sci* **67**: 191–196.

Gugler R, Manion CV, and Azarnoff DL (1976) Phenytoin: pharmacokinetics and bioavailability. *Clin Pharmacol Ther* **19**:135–142.

Hallifax D and Houston JB (2006) Binding of drugs to hepatic microsomes: comment and assessment of current prediction methodology with recommendation for improvement. *Drug Metab Dispos* **34**:724–726, author reply 727.

Hansch C, Leo A, and Hockman D (1995) *Exploring QSAR: Hydrophobic, Electronic, and Steric Constraints*, ACS Publications, Washington, DC.

Heizmann P, Eckert M, and Ziegler WH (1983) Pharmacokinetics and bioavailability of midazolam in man. *Br J Clin Pharmacol* **16** (Suppl 1):43S–49S.

Hermann P, Rodger SD, Remones G, Thenot JP, London DR, and Morselli PL (1983) Pharmacokinetics of diltiazem after intravenous and oral administration. *Eur J Clin Pharmacol* **24**: 349–352.

Hinderling PH (1997) Red blood cells: a neglected compartment in pharmacokinetics and pharmacodynamics. *Pharmacol Rev* **49**:279–295.

Hiskey CF, Bullock E, and Whitman G (1962) Spectrophotometric study of aqueous solutions of warfarin sodium. *J Pharm Sci* **51**:43–46.

Ishihama Y, Nakamura M, Miwa T, Kajima T, and Asakawa N (2002) A rapid method for pK_a determination of drugs using pressure-assisted capillary electrophoresis with photodiode array detection in drug discovery. *J Pharm Sci* **91**:933–942.

Jansson R, Bredberg U, and Ashton M (2008) Prediction of drug tissue to plasma concentration ratios using a measured volume of distribution in combination with lipophilicity. *J Pharm Sci* **97**: 2324–2339.

Jones RD, Jones HM, Rowland M, Gibson CR, Yates JWT, Chien JY, Ring BJ, Adkison KK, Ku MS, He H, et al. (2011) PhRMA CPCDC initiative on predictive models of human pharmacokinetics, part 2: comparative assessment of prediction methods of human volume of distribution. *J Pharm Sci* **100**:4074–4089.

Kochansky CJ, McMasters DR, Lu P, Koeplinger KA, Kerr HH, Shou M, and Korzekwa KR (2008) Impact of pH on plasma protein binding in equilibrium dialysis. *Mol Pharm* **5**: 438–448.

Korzekwa K and Nagar S (2014) Compartmental models for apical efflux by P-glycoprotein: part 2—a theoretical study on transporter kinetic parameters. *Pharm Res* **31**:335–346.

Korzekwa K and Nagar S (2017a) Drug distribution part 2. Predicting volume of distribution from plasma protein binding and membrane partitioning. *Pharm Res* **34**:544–551.

Korzekwa K and Nagar S (2017b) On the nature of physiologically-based pharmacokinetic models—A priori or a posteriori? Mechanistic or empirical? *Pharm Res* **34**: 529–534.

Kulkarni P, Korzekwa K, and Nagar S (2016) Intracellular unbound atorvastatin concentrations in the presence of metabolism and transport. *J Pharmacol Exp Ther* **359**:26–36.

Leo A, Hansch C, and Elkins D (1971) Partition coefficients and their uses. *Chem Rev* **71**:525–616.

Li R, Bi YA, Vildhede A, Scialis RJ, Mathialagan S, Yang X, Marroquin LD, Lin J, and Varma MVS (2017) Transporter-mediated disposition, clinical pharmacokinetics and cholestatic potential of glyburide and its primary active metabolites. *Drug Metab Dispos* **45**: 737–747.

Lombardo F, Obach RS, Dicapua FM, Bakken GA, Lu J, Potter DM, Gao F, Miller MD, and Zhang Y (2006) A hybrid mixture discriminant analysis—random forest computational model for the prediction of volume of distribution of drugs in human. *J Med Chem* **49**:2262–2267.

Lombardo F, Obach RS, Shalaeva MY, and Gao F (2004) Prediction of human volume of distribution values for neutral and basic drugs. 2. Extended data set and leave-class-out statistics. *J Med Chem* **47**:1242–1250.

Ludden TM, Boyle DA, Gieseker D, Kennedy GT, Crawford MH, Ludden LK, and Clementi WA (1988) Absolute bioavailability and dose proportionality of betaxolol in normal healthy subjects. *J Pharm Sci* **77**:779–783.

Maguire KP, Burrows GD, Norman TR, and Scoggins BA (1980) Blood/plasma distribution ratios of psychotropic drugs. *Clin Chem* **26**:1624–1625.

McAllister RG Jr and Kirsten EB (1982) The pharmacology of verapamil. IV. Kinetic and dynamic effects after single intravenous and oral doses. *Clin Pharmacol Ther* **31**:418–426.

Nagar S and Korzekwa K (2012) Commentary: nonspecific protein binding versus membrane partitioning: it is not just semantics. *Drug Metab Dispos* **40**:1649–1652.

Nagar S and Korzekwa K (2017) Drug distribution. Part 1. Models to predict membrane partitioning. *Pharm Res* **34**:535–543.

Nagar S, Korzekwa RC, and Korzekwa K (2017) Continuous intestinal absorption model based on the convection-diffusion equation. *Mol Pharm* **14**:3069–3086.

Nagar S, Tucker J, Weiskircher EA, Bhoopathy S, Hidalgo IJ, and Korzekwa K (2014) Compartmental models for apical efflux by P-glycoprotein—part 1: evaluation of model complexity. *Pharm Res* **31**:347–359.

Obach RS (1999) Prediction of human clearance of twenty-nine drugs from hepatic microsomal intrinsic clearance data: an examination of in vitro half-life approach and nonspecific binding to microsomes. *Drug Metab Dispos* **27**:1350–1359.

Obach RS, Baxter JG, Liston TE, Silber BM, Jones BC, MacIntyre F, Rance DJ, and Wastall P (1997) The prediction of human pharmacokinetic parameters from preclinical and in vitro metabolism data. *J Pharmacol Exp Ther* **283**:46–58.

Oie S and Tozer TN (1979) Effect of altered plasma protein binding on apparent volume of distribution. *J Pharm Sci* **68**:1203–1205.

O'Neil M (2006) *The Merck Index–An Encyclopedia of Chemicals, Drugs, and Biologicals*, Merck and Co., Inc., Whitehouse Station, NJ.

O'Reilly RA, Welling PG, and Wagner JG (1971) Pharmacokinetics of warfarin following intravenous administration to man. *Thromb Diath Haemorrh* **25**:178–186.

Pandey MM, Jaipal A, Kumar A, Malik R, and Charde SY (2013) Determination of pK_a of felodipine using UV-visible spectroscopy. *Spectrochim Acta A Mol Biomol Spectrosc* **115**: 887–890.

Poulin P and Haddad S (2011) Microsome composition-based model as a mechanistic tool to predict nonspecific binding of drugs in liver microsomes. *J Pharm Sci* **100**: 4501–4517.

Poulin P and Krishnan K (1995) A biologically-based algorithm for predicting human tissue: blood partition coefficients of organic chemicals. *Hum Exp Toxicol* **14**:273–280.

Poulin P, Schoenlein K, and Theil FP (2001) Prediction of adipose tissue: plasma partition coefficients for structurally unrelated drugs. *J Pharm Sci* **90**:436–447.

Poulin P and Theil FP (2000) A priori prediction of tissue:plasma partition coefficients of drugs to facilitate the use of physiologically-based pharmacokinetic models in drug discovery. *J Pharm Sci* **89**:16–35.

Poulin P and Theil FP (2002) Prediction of pharmacokinetics prior to in vivo studies. 1. Mechanism-based prediction of volume of distribution. *J Pharm Sci* **91**:129–156.

Poulin P and Theil FP (2009) Development of a novel method for predicting human volume of distribution at steady-state of basic drugs and comparative assessment with existing methods. *J Pharm Sci* **98**:4941–4961.

Recanatini M (1992) Partition and distribution coefficients of aryloxypropanolamine β-adrenoceptor antagonists. *J Pharm Pharmacol* **44**:68–70.

Regårdh CG, Borg KO, Johansson R, Johnsson G, and Palmer L (1974) Pharmacokinetic studies on the selective beta1-receptor antagonist metoprolol in man. *J Pharmacokinet Biopharm* **2**: 347–364.

Rekker R and Mannhold R (1992) *Calculation of Drug Lipophilicity: The Hydrophobic Fragmental Constant Approach*, VCH.

Riddell JG, Harron DWG, and Shanks RG (1987) Clinical pharmacokinetics of β-adrenoceptor antagonists. An update. *Clin Pharmacokinet* **12**:305–320.

Ripa S, Ferrante L, and Prenna M (1993) Pharmacokinetics of fluconazole in normal volunteers. *Chemotherapy* **39**:6–12.

Robinson MA and Mehvar R (1996) Enantioselective distribution of verapamil and norverapamil into human and rat erythrocytes: the role of plasma protein binding. *Biopharm Drug Dispos* **17**: 577–587.

Rodgers T, Leahy D, and Rowland M (2005) Physiologically based pharmacokinetic modeling 1: predicting the tissue distribution of moderate-to-strong bases. *J Pharm Sci* **94**:1259–1276.

Rodgers T and Rowland M (2006) Physiologically based pharmacokinetic modelling 2: predicting the tissue distribution of acids, very weak bases, neutrals and zwitterions. *J Pharm Sci* **95**: 1238–1257.

Rodgers T and Rowland M (2007) Mechanistic approaches to volume of distribution predictions: understanding the processes. *Pharm Res* **24**:918–933.

Rowland M and Tozer TN (2011) Distribution of drugs extensively bound to plasma proteins, *Clinical Pharmacokinetics and Pharmacodynamics: Concepts and Applications* pp 695–701, Wolters Kluwer Health/Lippincott William & Wilkins, Philadelphia, PA.

Sangster J (1993) *LOGKOW—A DataBank of Evaluated Octanol-Water Partition Coefficients*, Sangster Research Laboratories, Montreal, Canada.

Sangster J (1994) *Octanol-Water Partition Coefficients: Fundamentals and Physical Chemistry*, Wiley, New York.

Scavone JM, Luna BG, Harmatz JS, Von Moltke L, and Greenblatt DJ (1990) Diphenhydramine kinetics following intravenous, oral, and sublingual dimenhydrinate administration. *Biopharm Drug Dispos* **11**:185–189.

Stella VJ, Martodihardjo S, Terada K, and Rao VM (1998) Some relationships between the physical properties of various 3-acyloxymethyl prodrugs of phenytoin to structure: potential in vivo performance implications. *J Pharm Sci* **87**:1235–1241.

Tieleman DP, Marrink SJ, and Berendsen HJC (1997) A computer perspective of membranes: molecular dynamics studies of lipid bilayer systems. *Biochim Biophys Acta* **1331**: 235–270.

Uchimura T, Kato M, Saito T, and Kinoshita H (2010) Prediction of human blood-to-plasma drug concentration ratio. *Biopharm Drug Dispos* **31**:286–297.

Ueda CT, Hirschfeld DS, Scheinman MM, Rowland M, Williamson BJ, and Dzindzio BS (1976) Disposition kinetics of quinidine. *Clin Pharmacol Ther* **19**:30–36.

van De Waterbeemd H (1993) Calculation of Drug Lipophilicity – The Hydrophobic Fragmental Constant Approach. *Quantitative Structure-Activity Relationships* **12**:269-.

Waller ES, Sharanevych MA, and Yakatan GJ (1982) The effect of probenecid on nafcillin disposition. *J Clin Pharmacol* **22**:482–489.

Welker HA, Wiltshire H, and Bullingham R (1998) Clinical pharmacokinetics of mibefradil. *Clin Pharmacokinet* **35**:405–423.

Willis JV, Kendall MJ, and Jack DB (1980) A study of the effect of aspirin on the pharmacokinetics of oral and intravenous diclofenac sodium. *Eur J Clin Pharmacol* **18**: 415–418.

Wishart DS, Feunang YD, Guo AC, Lo EJ, Marcu A, Grant JR, Sajed T, Johnson D, Li C, Sayeeda Z, et al. (2018) DrugBank 5.0: a major update to the DrugBank database for 2018. *Nucleic Acids Res* **46** (D1):D1074–D1082.

Ye M, Nagar S, and Korzekwa K (2016) A physiologically based pharmacokinetic model to predict the pharmacokinetics of highly protein-bound drugs and the impact of errors in plasma protein binding. *Biopharm Drug Dispos* **37**:123–141.

Zhivkova Z and Doytchinova I (2012) Prediction of steady-state volume of distribution of acidic drugs by quantitative structure-pharmacokinetics relationships. *J Pharm Sci* **101**: 1253–1266.

Zou P, Zheng N, Yang Y, Yu LX, and Sun D (2012) Prediction of volume of distribution at steady state in humans: comparison of different approaches. *Expert Opin Drug Metab Toxicol* **8**: 855–872.

Address correspondence to: Ken Korzekwa, Temple University School of Pharmacy, 3307 N Broad St. Philadelphia, PA 19140. E-mail: korzekwa@temple.edu